

Studying Phase Transitions in Nuclear Collisions

I.N. Mishustin

*The Kurchatov Institute, Russian Research Center, 123182 Moscow, Russia;
The Niels Bohr Institute, Blegdamsvej 17, DK-2100 Copenhagen Ø, Denmark;
Institute for Theoretical Physics, J.-W. Goethe University, Robert-Meyer Str. 8-10,
D-60054 Frankfurt am Main, Germany*

Abstract

In this talk I discuss three main topics concerning the theoretical description and observable signatures of possible phase transitions in nuclear collisions. The first one is related to the multifragmentation of equilibrated sources and its connection to a liquid-gas phase transition in finite systems. The second one is dealing with the Coulomb excitation of ultrarelativistic heavy ions resulting in their deep disintegration. The third topic is devoted to the description of a first order phase transition in rapidly expanding matter. The resulting picture is that a strong collective flow of matter will lead to the fragmentation of a metastable phase into droplets. If the transition from quark-gluon plasma to hadron gas is of the first order, it will manifest itself by strong nonstatistical fluctuations in observable hadron distributions.

INTRODUCTION

A general goal of present and future experiments with heavy-ion beams is to study the properties of strongly interacting matter away from the nuclear ground state. The main interest is focussed on searching for and studying possible phase transitions. Several phase transitions are predicted in different domains of temperature T and baryon density ρ_B . There is no doubt that there should be a first order phase transition of the liquid-gas type in normal nuclear matter. This follows simply from the existence of the nuclear bound state at the saturation density $\rho_0 \approx 0.15 \text{ fm}^{-3}$. Therefore, at $\rho_B < \rho_0$ and low temperatures, $T < T_c \sim 10 \text{ MeV}$, the matter will organize itself in the form of a mixed phase with droplets of nuclear liquid surrounded by the nucleon gas. The only problem is whether relatively small amounts of excited nuclear matter produced in nuclear collisions and its limited lifetime are sufficient to observe this phase transition. Based on recent data on the nuclear caloric curve [1] and temperature fluctuations [2] I am tempting to give a positive answer to this question. This topic will be discussed in the first part of the

talk after a short description of the Statistical Multifragmentation Model (SMM) [3, 4] which provides a basis for theoretical analysis.

The situation at high T and nonzero baryon chemical potential μ ($\rho_B > 0$) is not so clear, although everybody is sure that the deconfinement and chiral transitions should occur somewhere. The phase structure of QCD is not yet fully understood. Reliable lattice calculations exist only for $\mu = 0$ ($\rho_B = 0$) where they predict a second order phase transition or crossover at $T \approx 160$ MeV. As model calculations show, the phase diagram in the (T, μ) plane may contain a first order transition line (below called the critical line) terminated at a (tri)critical point [5, 6]. Possible signatures of this point in heavy-ion collisions are discussed in ref. [7]. Under certain non-equilibrium conditions, a first order transition is also predicted for symmetric quark-antiquark matter [8].

A striking feature of central heavy-ion collisions at high energies, confirmed in many experiments (see e.g. [9, 10]), is a very strong collective expansion of matter. The applicability of equilibrium concepts for describing phase transitions under such conditions becomes questionable. In the last part of the talk I demonstrate that non-equilibrium phase transitions in rapidly expanding matter can lead to interesting phenomena which, in a certain sense, can be even easier to observe [11].

In the middle part of the talk I address a question which is closely related to the main topic of this conference. It illustrates how the knowledge accumulated in intermediate-energy heavy-ion physics can be used for ultrarelativistic heavy-ion colliders. Namely, I will discuss the excitation of nuclei by Lorentz-contracted and strongly-enhanced Coulomb fields of ultrarelativistic heavy ions. As well known, this process can be treated in terms of equivalent photons. Their flux grows linearly with the squared nuclear charge, and their characteristic energy is proportional to the relative Lorentz factor of colliding nuclei. This is why this Coulomb excitation of nuclei becomes especially important in high-energy heavy-ion colliders such as RHIC and LHC. The calculations [12, 13] show that in such colliders the equivalent photon spectrum extends far above the Giant Resonance region, into the GeV domain. The absorption of such a photon by a nucleus leads to its high excitation and subsequent disintegration. This might be an important factor determining a lifetime of ultrarelativistic heavy-ion beams.

STATISTICAL MULTIFRAGMENTATION AND LIQUID-GAS PHASE TRANSITION

When a nucleus is suddenly heated up to a temperature T it starts expanding to adjust a new equilibrium density $\rho_0(T)$ which is less than the equilibrium density at zero temperature ρ_0 . If the initial temperature is high enough the expansion is unlimited. At some stage of expansion the system enters into the spinodal region, where the homogeneous distribution of matter becomes thermodynamically unstable. Therefore, the nucleons form smaller and bigger clusters or droplets

with density close to ρ_0 . This clusterization process resembles a liquid-gas phase transition in ordinary fluids. In the transition region the matter is very soft in a sense that the sound velocity is close to zero (soft point). This means also that the expansion is slow and the system has enough time to find a most favorable cluster-size distribution maximizing the entropy.

At a later stage of expansion the system reaches a so-called freeze-out state when clusters cease to interact with each other. This break-up state of the system can be described within a statistical approach. In 1985 we have constructed a Statistical Multifragmentation Model (SMM) [3, 4] which up to now is one of the most successful realizations of this approach for finite nuclear systems. The model and its numerous applications are described in detail in a recent review [14]. A similar model was also constructed by Gross [15]. In this talk I outline only some general features of the SMM and give a few examples of how it works.

It is assumed that at break-up the system consists of primary hot fragments and nucleons in thermal equilibrium. Each break-up channel or partition, f , is specified by the multiplicities of different species, N_{AZ} , constrained by the total baryon number A_0 and charge Z_0 . The total fragment multiplicity is defined as $M = \sum_{AZ} N_{AZ}$. The probabilities of different break-up channels are calculated in an approximate microcanonical way according to their statistical weights,

$$W_f \propto \exp [S_f(E^*, V, A_0, Z_0)], \quad (1)$$

where S_f is the entropy of a channel f at excitation energy E^* and volume V .

Translational degrees of freedom of fragments are described by the Boltzmann statistics while the internal excitations of individual fragments with $A > 4$ are calculated according to the quantum liquid-drop model. An ensemble of microscopic states corresponding to a break-up channel f is characterized by a temperature T_f which is determined from the energy balance equation

$$\frac{3}{2}T(M-1) + \sum_{(A,Z)} E_{AZ}(T)N_{AZ} + E_f^C(V) - Q_f = E^* . \quad (2)$$

Here the first term comes from the translational motion, the second term includes internal excitation energies of individual fragments, the third term is the Coulomb interaction energy and the last one is the Q-value of the channel f . The excitation energy E^* is measured with respect to the ground state of the compound nucleus (A_0, Z_0) . It is fixed for all fragmentation channels while the temperature T_f fluctuates from channel to channel.

The total break-up volume is parametrized as $V = (1 + \kappa)V_0$, where V_0 is the compound nucleus volume at normal density and the model parameter κ is the same for all channels. The entropy associated with the translational motion of fragments is determined by the “free” volume, V_f , which is only a fraction of the total break-up volume V . In the SMM $V_f(M)$ is parametrized in such a way that it grows almost linearly with the primary fragment multiplicity M or equivalently, with the excitation energy $\varepsilon^* = E^*/A_0$ of the system [14].

At given inputs A_0 , Z_0 and ε^* the individual multifragment configurations are generated by the Monte Carlo method. After the break-up the hot primary fragments propagate in a common Coulomb field and loose their excitation. The most important de-excitation mechanisms included in the SMM [14] are the simultaneous Fermi break-up of lighter fragments ($A \leq 16$) and the evaporation from heavier fragments, including the compound-like residues. In refs. [17, 18, 19, 20, 21, 22] one can find fresh examples showing how well the SMM works in describing the multifragmentation of thermalized sources.

In ref. [16] an equation of state of a multifragment system was calculated for the grand canonical version of the SMM. As expected, it shows clear signs of a liquid-gas phase transition with a critical temperature of about 7 MeV. In the transition region the pressure isotherms are very flat indicating that the sound velocity is very small. In this region the compressibility and specific heat have nonmonotonic behaviour.

The most interesting prediction of the statistical model, a plateau in the caloric curve $T(\varepsilon^*)$, was formulated already in 1985 [23]. Since that time it was a challenge for experimentalists to measure the nuclear caloric curve. First measurements were performed at GSI by the ALADIN collaboration only in 1995 [24]. They have shown an impressive agreement with the theoretical prediction. These results have initiated an avalanche of other measurements and a lively discussion in the community (see latest ALADIN results in ref. [25]).

Most temperature measurements are based on the Albergo method [26] relating the temperature to the double ratio of isotope yields. The analysis shows (see for instance [1, 27]) that the temperatures extracted by this method are very sensitive to the side-feeding and nuclear structure effects. According to SMM the observed light isotopes are produced mainly by the secondary decays of hot primary fragments. This leads to a difference between the isotopic temperatures and true thermodynamical temperature at freeze-out (see detailed analysis in ref. [1]). In particular, isotopic temperatures have typically a less pronounced plateau than the true temperature, which can even have a backbending. In recent years several comparisons have been made (see examples in refs. [1, 18, 28]) which generally show very good agreement between the theory and experiment.

One should bear in mind that the ALADIN caloric curves are measured for a wide ensemble of decaying sources associated with the projectile or target spectators produced in peripheral nuclear collisions. The thermodynamical significance of such observations would increase if the measurements were done for a fixed source size with a varying excitation energy. Also the temperature measurements on the event-by-event basis would make it possible to study its fluctuations and therefore the heat capacity of the nuclear system. Such an analysis was performed recently by the Bologna group [2] in the study of quasi-projectile (QP) fragmentation in peripheral Au+Au collisions at 35 A MeV. In this analysis only the events with reconstructed QP charges $70 < Z_{QP} < 88$ were included. The excitation energy, determined by a calorimetric method, varied for these events from 0.5 to about 8

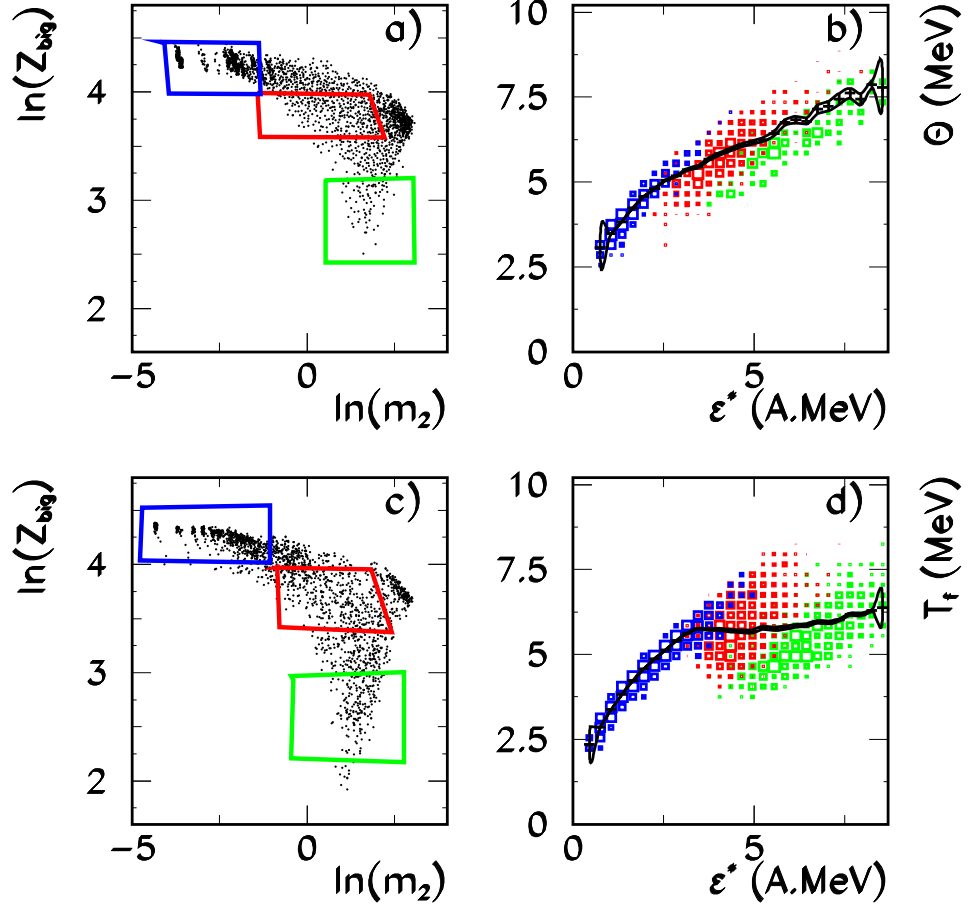


Figure 1: Experimental (a) and SMM generated (c) Campi scatter plots. Three cuts are introduced to select liquid-like events (Cut 1), gas-like events (Cut 3) and critical events (Cut 2). Panels (b) and (d) show the correlation between temperatures and excitation energies for experimental and SMM generated events. Events belonging to different cuts are shown by blue (1), red (2) and green (3) squares. Sizes of the squares are proportional to the yields. The solid lines in panels (b) and (d) show the mean temperatures for all the events at given ϵ^* .

MeV/nucleon.

Measuring temperatures event by event is of course a nontrivial task. An attempt of estimating the event “temperature” (below denoted by θ) was made in ref. [2]. The idea is to apply the energy balance equation (2), which is used in the SMM, but now for the experimental events. Of course, this requires certain assumptions on how the observed partitions, involving cold reaction products, are related to the original partitions consisting of hot primary fragments. Therefore, it was assumed that the light particles detected in a partition were produced by de-excitation of hot primary fragments. For reconstructing a primary partition these light particles were shared among the detected fragments proportionally to their charges and assuming the charge-to-mass ratio as in the entrance channel. Applying this procedure for the asymptotic SMM events showed that the correlation between the microcanonical temperature and excitation energy was reproduced within 5%.

Fig. 1 shows the scatter plots in the (T, ε^*) plane for experimental (b) and SMM generated (d) events. The ensemble-averaged temperatures are indicated by the solid lines. Their behaviour is typical for caloric curves measured by other methods. In addition to the flattening of the average temperature at $T \approx 6$ MeV, one can clearly see the broadening of the distributions in the transition region at $\varepsilon^* = 4 \div 8$ MeV/nucleon. The quantity characterizing energy fluctuations is heat capacity. For a canonical ensemble at constant volume it can be expressed as

$$C_V = \frac{\sigma_E^2}{T^2} = \frac{\langle E^2 \rangle - \langle E \rangle^2}{T^2}. \quad (3)$$

It is not clear whether the constant volume condition applies to actual freeze-out configurations but nevertheless studying the energy fluctuations provides an additional and important information compared to the average characteristics. Indeed, applying Eq. (3) for scatter plots of Fig. 1 reveals a peak in C_V at temperatures around 6 MeV. This behaviour was also predicted theoretically a long time ago [23, 15].

Another way of characterizing the critical behaviour is to analyze the conditional moments of fragment multiplicity distributions introduced by Campi [29]. Fig. 1 a) shows, for each event j , the experimental correlation between the logarithm of the charge of the largest fragment, $\ln(Z_{big}^{(j)})$, and the logarithm of the corresponding second moment of the multiplicity distribution, $\ln(m_2^{(j)})$ (Campi scatter plot). Fig. 1 c) shows the same for events generated by the SMM. As expected for a system experiencing a phase transition these plots exhibit two branches: an upper branch with an average negative slope, corresponding to under-critical events, and a lower branch with a positive slope that corresponds to super-critical events. The two branches meet in a central region signalling the approach to a critical point. This trend is nicely reproduced in Fig. 1 by both the experiment and the theory.

We have made three cuts in these scatter plots selecting the upper branch (Cut 1), the lower branch (Cut 3) and the central region (Cut 2) and analyzed the events falling in each of the three zones. The fragment charge distributions in

these three zones exhibit shapes going from a U-shape in Cut 1, characteristic of the evaporation events at low excitation energies, to an exponential one in Cut 3, characteristic of the vaporization events at high excitations. In Cut 2 a power-law fragment charge distribution $Z^{-\tau}$ with $\tau \approx 2.2$ is observed as expected according to the Fisher's droplet model for fragment formation near the critical point of a liquid-gas phase transition [30] (see also an interesting analysis of ref. [22]).

The contributions of these three types of events to the caloric curves are shown in Fig. 1 for experiment (b) and for theory (d). It is clearly seen for both the data and the SMM, that in Cuts 1 and 3 besides normal events there are unusual events (although with low probability) which lie far from the average $T(\varepsilon^*)$ behaviour. These are compound-like states with very high temperatures and vaporization events with low temperatures. For these events one can make the analogy respectively with an overheated liquid and a super-cooled gas in the ordinary liquid-gas phase transition. Here we see the advantage of a finite system where not only the most probable states but also the metastable states can be produced with a finite probability. In my opinion, the observation of these metastable states is the best indication that we are dealing here with the first order phase transition of the liquid-gas type. These interesting questions were further studied in ref. [31].

ELECTROMAGNETIC EXCITATION OF ULTRARELATIVISTIC HEAVY IONS

It has become clear in recent years [12, 13] that high nuclear excitations can be induced by the Coulomb fields of ultrarelativistic heavy ions. Following the famous Waizsäcker-Williams method the Lorentz contracted Coulomb field of an ultrarelativistic projectile in the rest frame of a target nucleus (and vice versa) can be represented as a beam of equivalent or virtual photons. The flux of equivalent photons with energy E_γ in a collision of nuclei with charge Z at impact parameter b is given by the standard formula

$$N(E_\gamma, b) = \frac{\alpha Z^2}{\pi^2} \frac{x^2}{\beta^2 E_\gamma b^2} \left[K_1^2(x) + \frac{1}{\gamma^2} K_0^2(x) \right], \quad (4)$$

where α is the fine structure constant, $\beta = v/c$ and $\gamma = \sqrt{1 - \beta^2}$ is the relative Lorentz factor. The variable x in the modified Bessel functions $K_{0,1}(x)$ is defined as $x = E_\gamma b / (\beta \gamma \hbar c)$. Since $K_{0,1}$ drop exponentially at large arguments, the main contribution to the virtual photon flux comes from the region $x \sim 1$. Thus the characteristic energy of virtual photons grows linearly with γ . This explains why the relativistic Coulomb excitation is very important for ultrarelativistic heavy-ion beams where both γ and Z are large. For colliding beams $\gamma = 2\gamma_{beam}^2 - 1$ that gives $2 \cdot 10^4$ and 10^7 for RHIC and LHC respectively. This brings the spectrum of virtual photons into the GeV energy domain, i. e. much above the traditionally studied Giant Resonance (GR) and Delta-resonance regions. The absorption of

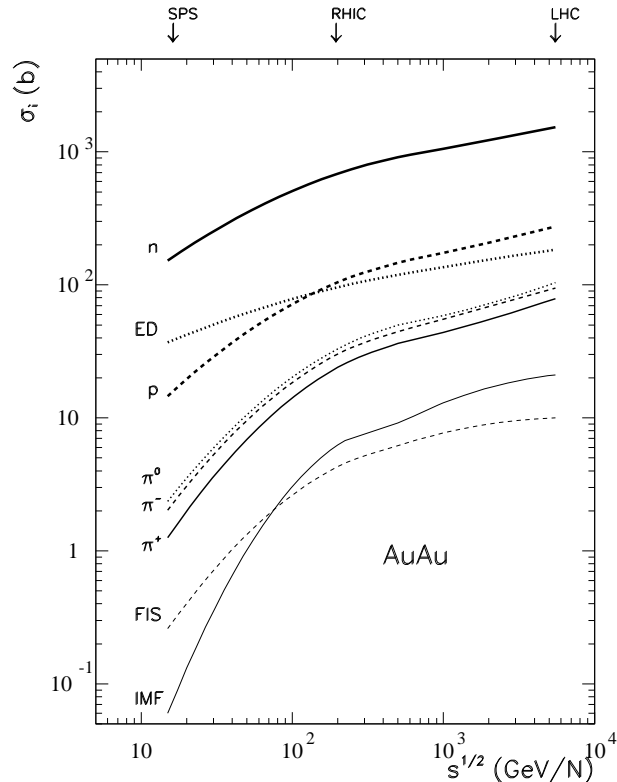


Figure 2: Theoretical predictions for inclusive cross sections for emitting nucleons, pions, intermediate mass fragments (IMF: $3 \leq Z \leq 30$) and fission fragments (FIS: $30 < Z \leq 50$) in the electromagnetic dissociation of Au nuclei as functions of the c.m. energy \sqrt{s} (the SPS, RHIC and LHC energies are indicated by arrows). The thick dotted line shows the total ED cross section for Au beams.

such a high-energy photon will result in a very high nuclear excitation sufficient for its total disintegration.

In ref. [32] the description of nuclear photoabsorption was extended to the photon energies much above the GR region, where the excitation of individual nucleons and multiple pion production are the dominant reaction channels. A model of electromagnetic dissociation (ED) taking into account these high-energy photon absorption channels was constructed in ref. [12]. According to this model, the fast hadrons produced after the photon absorption initiate a cascade of subsequent collisions with the intranuclear nucleons leading to the fast particle emission and heating of a residual nucleus. This stage is described by the Intranuclear Cascade Model (INC). At a later stage the nucleus undergoes de-excitation by means of the evaporation of nucleons and lightest fragments, binary fission or multifragmentation. The latter process becomes important at ultrarelativistic beam energies, when the excitation energy of residual nuclei exceeds 3-4 MeV/nucleon. This stage of the reaction is described by the SMM.

To include all the processes described above, in ref. [13] we have developed a specialized computer code RELDIS aimed at the Monte Carlo simulation of the Relativistic ELectromagnetic DISsociation of nuclei. The simulation begins with generating the single- or double-photon absorption process. Then the INC model is used to calculate the fast particle emission and the characteristics of residual nuclei. Finally, de-excitation of thermalized residual nuclei is simulated by the SMM.

The cross section of the photo-nuclear (γA) reaction induced by a photon of energy E_γ is expressed as

$$\frac{d\sigma_{ED}}{dE_\gamma} = \sigma_{\gamma A}(E_\gamma) \int_{b_{min}}^{\infty} N(E_\gamma, b) 2\pi b db, \quad (5)$$

where $b_{min} \approx (R_p + R_t)$ is a minimal impact parameter for heavy-ion collisions without nuclear overlap, $\sigma_{\gamma A}(E_\gamma)$ is an appropriate photo-absorption cross section, either measured for the A -nucleus with real photons or calculated within a model. The total ED cross section, σ_{ED} , is obtained by integrating Eq. (5) by dE_γ from 0 to ∞ . The calculations [12] show that the total ED cross sections for RHIC and LHC are very large, 100 b and 200 b respectively. Accordingly, the ED reaction rates are much higher than those for nuclear interactions, although the ED events are much less violent. For instance, at expected RHIC luminosity $L \approx 10^{27} \text{ cm}^{-2}\text{s}^{-1}$ the ED reaction rate will be 10^5 interactions per second. Together with the electron capture reactions the ED processes will be the important factors reducing the lifetime of ultrarelativistic heavy-ion beams compared with the proton ones.

We have applied the RELDIS code for calculating the ED characteristics for several heavy-ion beams. The model is in a reasonable agreement with experimental data, when available. We have also made predictions for the reactions: 160A GeV Pb+Pb (SPS), 100A+100A GeV Au+Au (RHIC) and 2.75A+2.75A TeV Pb+Pb (LHC). The inclusive (multiplicity weighted) cross sections for emitting nucleons, pions and nuclear fragments in the electromagnetic dissociation of one of the colliding Au nuclei are shown in Fig. 2 as functions of the incident c.m. energy. Nuclear fragments are divided in two groups: fission fragments ($30 < Z \leq 50$) and Intermediate Mass Fragments (IMFs, $3 \leq Z \leq 30$), which are associated with the multifragmentation. One can clearly see a steep rise in the yields of all species, especially IMFs, when the incident energy grows from the SPS to RHIC and LHC domain. The inclusive cross section for neutron emission is especially large, above 1000 b at RHIC and LHC. The average neutron multiplicities are predicted to be 4.1, 7.2 and 8.8 at SPS, RHIC and LHC respectively.

The predicted neutron multiplicity distributions are shown in Fig. 3. They have a nontrivial structure. There is a strong peak at 1n emission channel associated with the GR decay. On the other hand, there is a long tail of multiple neutron emission associated with more violent reaction channels, from the direct knock-out and evaporation from the compound nucleus to fission and multifragmentation. This is where our model including all these channels shows its strength. One can see, for example, that the probability to emit more than 20 neutrons is quite noticeable

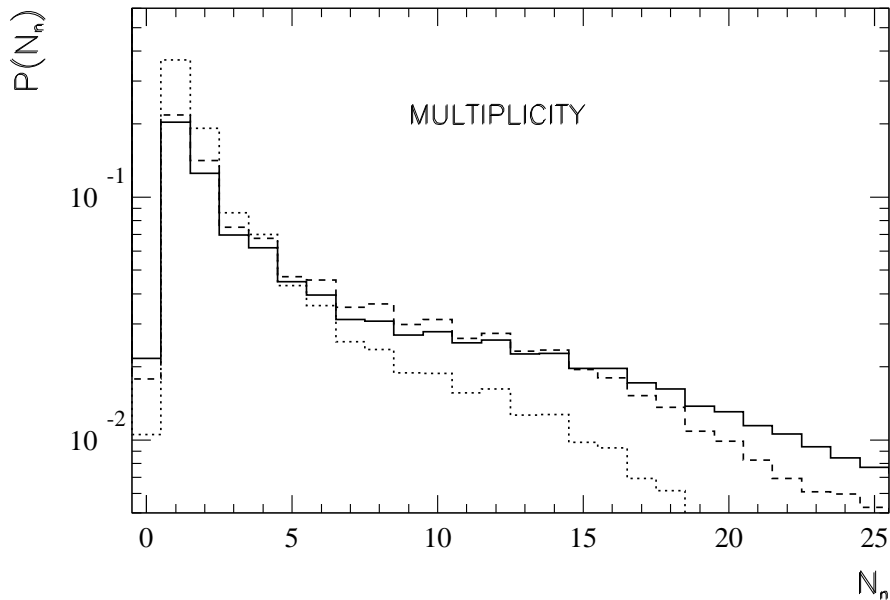


Figure 3: Normalized neutron multiplicity distributions for the electromagnetic dissociation of Pb nuclei at LHC and SPS (solid and dotted histograms, respectively) and Au nuclei at RHIC energies (dashed histogram). Calculations are made with RELDIS code.

($\approx 5\%$ at RHIC). These results might be important for designing neutron-sensitive zero-degree calorimeters at RHIC and LHC. One of such proposals was made recently in ref. [33] but only the 1n channel was considered there.

FIRST ORDER PHASE TRANSITION IN FAST DYNAMICS

The implications of a strong collective expansion on the liquid-gas phase transition were discussed in ref. [34]. Here I will focus on consequences of the strong collective flow of matter for a possible first order chiral transition. I will assume that the collective velocity field is described locally by the Hubble law, $v(r) = H \cdot r$, where the Hubble “constant” H may in general depends on time.

To make the discussion more concrete, I adopt a picture of the chiral phase transition predicted by the linear sigma-model with constituent quarks [35]. Then the mean chiral field $\Phi = (\sigma, \pi)$ serves as an order parameter. The model respects chiral symmetry, which is spontaneously broken in the vacuum where $\sigma = f_\pi$, $\pi = 0$. The effective thermodynamic potential $\Omega(T, \mu; \Phi)$ depends, besides Φ , on temperature T and baryon chemical potential μ . The schematic behaviour of $\Omega(T, \mu; \Phi)$ as a function of the order parameter field σ at $\pi = 0$ is shown in Fig. 4. The minima of Ω correspond to the stable or metastable states of matter under the

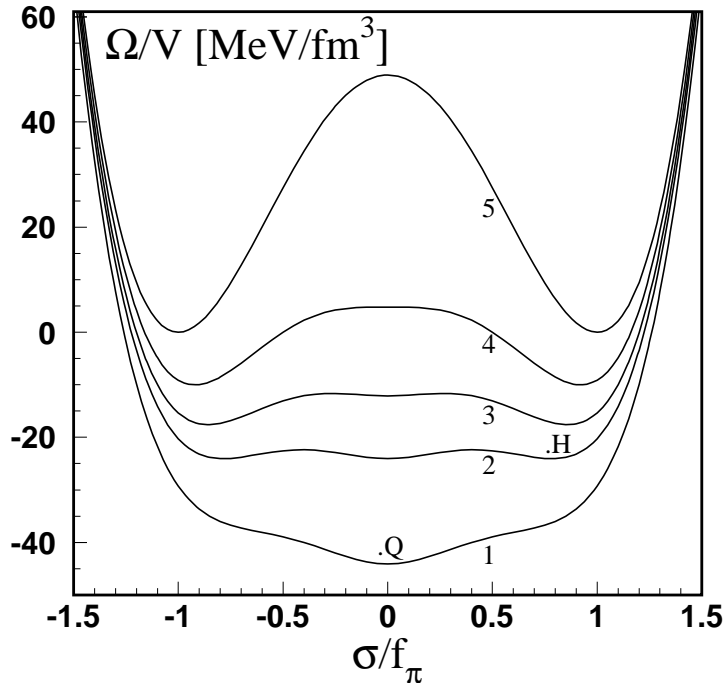


Figure 4: Schematic view of the effective thermodynamic potential per volume Ω/V as a function of the order parameter field σ at $\pi = 0$, as predicted by the linear σ -model in the chiral limit $m_\pi = 0$ [35]. The curves from bottom to top correspond to the different stages of the isentropic expansion of homogeneous matter starting from $T=100$ MeV and $\mu=750$ MeV (curve 1). The upper curve 5 is the vacuum potential. The other curves are discussed in the text.

condition of thermodynamical equilibrium, where the pressure is $P = -\Omega_{min}/V$. The curves from bottom to top correspond to different stages of the isentropic expansion of homogeneous matter. Each curve represents a certain point on the (T, μ) trajectory. As one can see from the figure, the model of ref. [35] reveals a rather weak first order phase transition, although some other models [5, 6] predict a stronger transition. The discussion below is quite general.

Assume that at some early stage of the reaction the thermal equilibrium is established, and partonic matter is in a “high energy density” phase Q. This state corresponds to the absolute minimum of Ω with the order parameter close to zero, $\sigma \approx 0$, $\pi \approx 0$, and chiral symmetry restored (curve 1). Due to a very high internal pressure, Q matter will expand and cool down. At some stage a metastable minimum appears in Ω at a finite value of σ corresponding to a “low energy density” phase H, in which chiral symmetry is spontaneously broken. At some later time, the critical line in the (T, μ) plane is crossed where the Q and H minima have equal depths, i.e. $P_H = P_Q$ (curve 2). At later times the H phase becomes more favorable (curve 3), but the two phases are still separated by a potential barrier. If the expansion of the Q phase continues until the barrier vanishes (curve 4), the system will find itself in an absolutely unstable state at a maximum of the thermodynamic potential. Therefore, it will freely roll down into the lower energy state

corresponding to the H phase. This situation is known as a spinodal instability.

As well known, a first order phase transition proceeds through the nucleation process. According to the standard theory of homogeneous nucleation [36], supercritical bubbles of the H phase appear only below the critical line, when $P_H > P_Q$. In rapidly expanding matter the nucleation picture might be very different. As shown in ref. [11], the phase separation in this case can start as early as the metastable H state appears in the thermodynamic potential, and a stable interface between the two phases may exist. An appreciable amount of nucleation bubbles and even empty cavities may be created already above the critical line.

The bubble formation and growth will also continue below the critical line. Previously formed bubbles will now grow faster due to increasing pressure difference, $P_H - P_Q > 0$, between the two phases. It is most likely that the conversion of Q matter on the bubble boundary is not fast enough to saturate the H phase. Therefore, a fast expansion may lead to a deeper cooling of the H phase inside the bubbles compared to the surrounding Q matter. Strictly speaking, such a system cannot be characterized by the unique temperature. At some stage the H bubbles will percolate, and the topology of the system will change to isolated regions of the Q phase (Q droplets) surrounded by the undersaturated vapor of the H phase.

The characteristic droplet size can be estimated by applying the energy balance consideration, proposed by Grady [37, 38] in the study of dynamical fragmentation of fluids. The idea is that the fragmentation of expanding matter is a local process minimizing the sum of surface and kinetic (dilatational) energies per fragment volume. As shown in ref. [34], this prescription works fairly well also for multifragmentation of expanding nuclei, where the standard statistical approach fails.

Let us imagine an expanding spherical Q droplet of radius R , embedded in the background of the dilute H phase. The change of the thermodynamic potential, $\Delta\Omega$, compared to the uniform H phase can be easily estimated within the thin-wall approximation [11]. According to the Grady's prescription, the quantity to be minimized is $\Delta\Omega$ per droplet volume, $V \propto R^3$, that is

$$\left(\frac{\Delta\Omega}{V}\right)_{droplet} = -(P_Q - P_H) + \frac{3\gamma}{R} + \frac{3}{10}\Delta\mathcal{E}H^2R^2. \quad (6)$$

Here $\Delta\mathcal{E} = \mathcal{E}_Q - \mathcal{E}_H$ is the difference of the bulk energy densities of the two phases, γ is the interface energy per unit area. One should notice that the last term, i.e. the change in the collective kinetic energy, is positive because $\mathcal{E}_Q > \mathcal{E}_H$. This term acts here as an effective long-range potential, similar to the Coulomb potential in nuclei. Since the bulk term does not depend on R the minimization condition constitutes the balance between the collective kinetic energy and the interface energy. This leads to an optimum droplet radius

$$R^* = \left(\frac{5\gamma}{\Delta\mathcal{E}H^2}\right)^{1/3}. \quad (7)$$

One can say that the metastable Q phase is torn apart by a mechanical strain associated with the collective expansion. This phenomenon has a direct analogy

with the fragmentation of pressurized fluids leaving nozzles [39, 40]. In a similar way, splashed water forms droplets which have little to do with the equilibrium liquid-gas phase transition.

In the lowest-order approximation the characteristic droplet mass can be calculated as $M^* \approx \Delta\mathcal{E}V$. It is natural to think that nucleons and heavy mesons are smallest droplets of the Q phase. For numerical estimates I take $\gamma = 10 \text{ MeV}/\text{fm}^2$ and $\Delta\mathcal{E} = 0.5 \text{ GeV}/\text{fm}^3$, i.e. the energy density inside the nucleon. For the Hubble constant I consider two possibilities: $H^{-1} = 20 \text{ fm}/c$, representing a slow expansion from a soft point, and $H^{-1} = 6 \text{ fm}/c$ typical for a fast expansion. Substituting these values in Eq. (7) one gets $R^* = 3.4 \text{ fm}$ and 1.5 fm for the slow and fast expansion respectively. These two values of R^* give M^* of about 100 GeV and 10 GeV , respectively. At ultrarelativistic energies the collective expansion is very anisotropic, with the strongest component along the beam axes. For the predominantly 1-d expansion one should expect the formation of slab-like structures with intermittent layers of Q and H phases.

After separation the droplets recede from each other according to the global Hubble expansion, predominantly along the beam direction. Hence their center-of-mass rapidities are in one-to-one correspondence with their spatial positions. Presumably they will be distributed more or less evenly between the target and projectile rapidities. Since rescatterings in the dilute H phase are rare, most hadrons produced from individual droplets will go directly into detectors. One can guess that the number of produced hadrons is proportional to the droplet mass. Each droplet will give a bump in the hadron rapidity distribution around its center-of-mass rapidity. If emitted particles have a Boltzmann spectrum, the width of the bump will be $\delta y \sim 2\sqrt{T/m}$, where T is the droplet temperature and m is the particle mass. At $T \sim 100 \text{ MeV}$ this gives $\delta y \approx 2$ for pions and $\delta y \approx 1$ for nucleons. These spectra might be slightly modified by the residual expansion of droplets and their transverse motion. The resulting rapidity distribution in a single event will be a superposition of contributions from different droplets, and therefore it will exhibit strong non-statistical fluctuations. The fluctuations will be more pronounced if primordial droplets are big, as expected in the vicinity of the soft point. If droplets as heavy as 100 GeV are formed, each of them will emit up to ~ 300 pions within a narrow rapidity interval, $\delta y \sim 1$. Such bumps can be easily resolved and analyzed. The fluctuations will be less pronounced if many small droplets shine in the same rapidity interval. Critical fluctuations of similar nature were discussed in ref. [41].

Some unusual events produced by high-energy cosmic nuclei have been already seen by the JACEE collaboration [42]. Unfortunately, they are very few and it is difficult to draw definite conclusions by analyzing them. We should be prepared to see plenty of such events in the future RHIC and LHC experiments. It is clear that the nontrivial structure of the hadronic spectra will be washed out to a great extent when averaging over many events. Therefore, more sophisticated methods of the event sample analysis should be used. The simplest one is to search for non-statistical fluctuations in the hadron multiplicity distributions measured

in a fixed rapidity bin [43]. One can also study the correlation of multiplicities in neighbouring rapidity bins, bump-bump correlations etc. Such standard methods as intermittency and cumulant moments [41], wavelet transforms [44], HBT interferometry [45] can also be useful. All these studies should be done at different collision energies to identify the phase transition threshold. The predicted dependence on the Hubble constant and the reaction geometry can be checked in collisions with different ion masses and impact parameters.

CONCLUSIONS

- The statistical approach (SMM) works well in situations when thermalized sources are well defined and no significant collective flow is present.
- The quantitative agreement of SMM with recent data on the caloric curve and temperature fluctuations provides a strong indication on the nuclear liquid-gas phase transition. The nuclear heat capacity has a peak at $T \approx 6$ MeV.
- A first order phase transition in rapidly expanding matter should proceed through the nonequilibrium stage when a metastable phase splits into droplets. The primordial droplets should be biggest in the vicinity of a soft point when the expansion is slowest.
- Hadron emission from droplets of the quark-gluon plasma should lead to large nonstatistical fluctuations in their rapidity spectra and multiplicity distributions. The hadron abundances may reflect directly the chemical composition in the plasma phase.
- Electromagnetic excitation of nuclei in ultrarelativistic heavy-ion colliders is an important reaction mechanism leading to the deep nuclear disintegration. The multiple neutron emission associated with this process may be used for monitoring ultrarelativistic heavy-ion beams.
- And finally, we should use the lessons of the liquid-gas phase transition for future studies of the deconfinement-hadronization and chiral phase transitions in relativistic heavy-ion collisions.

ACKNOWLEDGMENTS

The author is grateful to J.P. Bondorf and A.D. Jackson for many fruitful discussions. I thank A.S. Botvina, M. D'Agostino, A. Mocsy, I.A. Pshenichnov, O. Scavini for cooperation. Discussions with D. Diakonov, A. Dumitru, J.J. Gaardhoje, M.I. Gorenstein, W. Greiner, B. Jakobsson, L. McLerran, R. Mattiello, W.F.J. Müller, W. Reisdorf, L.M. Satarov, H. Stöcker, E.V. Shuryak, W. Trautmann and

V. Viola are greatly appreciated. I thank the Niels Bohr Institute, Copenhagen University, and the Institute for Theoretical Physics, Frankfurt University, for kind hospitality. This work was carried out partly within the framework of a Humboldt Award, Germany.

References

- [1] J.P. Bondorf, A.S. Botvina and I.N. Mishustin, *Phys. Rev.* **C58**, R27 (1998).
- [2] M. D'Agostino, A.S. Botvina, M. Bruno, A. Bonasera, J.P. Bondorf, I.N. Mishustin, F. Gulminelli, R. Bougault, N. Le Neindre, P. Desesquelles, E. Geraci, A. Pagano, I. Iori, A. Moroni, G.V. Margagliotti, G. Vannini, *Nucl. Phys.* **A650**, 329 (1999).
- [3] J.P. Bondorf, R. Donangelo, I.N. Mishustin, C.J. Pethick, H. Schulz, K. Sneppen, *Nucl. Phys.* **A443**, 321 (1985).
- [4] I.N. Mishustin, *Nucl. Phys.* **A 447** (1985) 67c.
- [5] J. Berges and K. Rajagopal, *Nucl. Phys.* **B538**, 215 (1999).
- [6] M.A. Halasz, A.D. Jackson, R.E. Shrock, M.A. Stephanov and J.J.M. Verbarshot, *Phys. Rev.* **D58**, 096007 (1998).
- [7] M. Stephanov, K. Rajagopal and E. Shuryak, *Phys. Rev. Lett.* **81**, 4816 (1998).
- [8] I.N. Mishustin, L.M. Satarov, H. Stoecker and W. Greiner, *Phys. Rev.* **C59**, 3243 (1999).
- [9] W. Reisdorf and FOPI Collaboration, *Nucl. Phys.* **A612**, 493 (1997).
- [10] P. Braun-Münzinger and J. Stachel, *Nucl. Phys.* **A638**, 3c (1998).
- [11] I.N. Mishustin, *Phys. Rev. Lett.* **82**, 4779 (1999).
- [12] I.A. Pshenichnov, I.N. Mishustin, J.P. Bondorf, A.S. Botvina, A.S. Iljinov, *Phys. Rev.* **C57**, 1920 (1998).
- [13] I.A. Pshenichnov, I.N. Mishustin, J.P. Bondorf, A.S. Botvina, A.S. Iljinov, *Phys. Rev.* **C60**, 044901 (1999).
- [14] J.P. Bondorf, A.S. Botvina, A.S. Iljinov, I.N. Mishustin and K.Sneppen, *Phys. Rep.* **257** (1995) 133.
- [15] D.H.E. Gross, *Rep. Progr. Phys.* **53** (1990) 605.
- [16] S. Das Gupta, J. Pan, I. Kvasnikova, C. Gale, *Nucl. Phys.* **A621**, 897 (1997).
- [17] A.S. Botvina et al., *Nucl. Phys.* **A584** (1995) 737.
- [18] H. Xi and ALADIN Collaboration, *Z. Phys.* **A359**, 397 (1997).
- [19] M. D'Agostino et al., *Phys. Lett.* **B371**,175 (1996).
- [20] R. Bougault et al., in *Proceedings of the XXXV International Winter Meeting on Nuclear Physics (Bormio, February 3-7, 1997)*; Preprint LPCC 97-04, April 1997.

- [21] V.E. Viola et al., in *Proceedings of the International Workshop on Gross Properties of Nuclei and Nuclear Excitations XXVII: Multifragmentation (Hirschegg, Austria, 17-23 January 1999)*, p. 93; Preprint INC-40007-136, Indiana University, 1999.
- [22] R.P. Scharenberg, B.K. Srivastava and EOS Colaboration, in the same *Hirschegg Proceedings as above*, pp. 237, 247.
- [23] J.P. Bondorf, R. Donangelo, I.N. Mishustin, H. Schulz, *Nucl. Phys.* **A444**, 460 (1985).
- [24] J. Pochodzalla and ALADIN Collaboration, *Phys. Rev. Lett.* **75**, 1040 (1995).
- [25] W.F.J. Müller, in the same *Hirschegg Proceedings as above*, p. 200.
- [26] S. Albergo et al., *Nuovo Cimento* **89**, 1 (1985).
- [27] M.B. Tsang, W.G. Lynch, H. Xi and W.A. Friedman, *Phys. Rev. Lett.* **78** 3836 (1997).
- [28] Al. H. Raduta, Ad.R. Raduta, *Phys. Rev.* **C59**, 323 (1999).
- [29] X. Campi, *J. Phys.* **A19**, L917 (1986); *Phys. Lett.* **B208**, 351 (1988).
- [30] M.E. Fisher, *Rep. Prog. Phys.* **30**, 615 (1967).
- [31] F. Gulminelli and Ph. Chomaz, *Phys. Rev. Lett.* **82**, 1402 (1999).
- [32] A.S. Iljinov, I.A. Pshenichnov, N. Bianchi, E. De Sanctis, V. Muccifora, M. Mirazita and P. Rossi, *Nucl. Phys.* **A616**, 575 (1997).
- [33] A.J. Baltz, C. Chasman, and S.N. White, nucl-ex/9801002.
- [34] I.N. Mishustin, in *Proceedings of the 6th International Conference on Nucleus-Nucleus Collisions (Gatlinburg, June 2-6, 1997)*; *Nucl. Phys.* **A630**, 111c (1998).
- [35] L.P. Csernai, I.N. Mishustin and A. Mocsy, *Heavy Ion Phys.*, **3**, 151 (1996); A. Mocsy, M.Sc. thesis, University of Bergen, 1996.
- [36] L.P. Csernai, J.I. Kapusta, *Phys. Rev. Lett.* **69**, 737 (1992); *Phys. Rev.* **D46**, 1379 (1992).
- [37] D.E. Grady, *J. Appl. Phys.* **53**(1), 322 (1981).
- [38] B.L. Holian and D.E. Grady, *Phys. Rev. Lett.* **60**, 1355 (1988).
- [39] J.A. Blink and W.G. Hoover, *Phys. Rev.* **A32**, 1027 (1985).
- [40] H. Buchenau et al., *J. Chem. Phys.* **92**, 6875 (1990).
- [41] N.G. Antoniou, *Nucl. Phys.* **B71**, 307 (1999).
- [42] T.H. Barnett et al., *Phys. Rev. Lett.* **50**, 2062 (1983).
- [43] M.J. Tannenbaum and E802 Collaboration, *Phys. Rev.* **C52**, 2663 (1995)
- [44] N. Suzuki, M. Biyajima and A. Ohsawa, hep-ph/9503403.
- [45] H. Heiselberg, A.D. Jackson, hep-ph/9809013.